Separation Science and Technology
Publication details, including instructions for authors and subscription information:
http://www.informaworld.com/smpp/title~content=t713708471

AGGREGATION OF DIALKYL-SUBSTITUTED DIPHOSPHONIC ACIDS AND ITS EFFECT ON METAL ION EXTRACTION

R. Chiarizia[a]; R. E. Barrans Jr.[a]; J. R. Ferraro[a]; A. W. Herlinger[b]; D. R. McAlister[b]
[a] Chemistry Division, Argonne National Laboratory*, Argonne, Illinois, U.S.A. [b] Chemistry Department, Loyola University Chicago, Chicago, Illinois, U.S.A.

Online publication date: 30 June 2001

To cite this Article Chiarizia, R. , Barrans Jr., R. E. , Ferraro, J. R. , Herlinger, A. W. and McAlister, D. R.(2001) 'AGGREGATION OF DIALKYL-SUBSTITUTED DIPHOSPHONIC ACIDS AND ITS EFFECT ON METAL ION EXTRACTION', Separation Science and Technology, 36: 5, 687 — 708
To link to this Article: DOI: 10.1081/SS-100103615
URL: http://dx.doi.org/10.1081/SS-100103615

SEPARATION SCIENCE AND TECHNOLOGY, 36(5&6), 687–708 (2001)

AGGREGATION OF DIALKYL-SUBSTITUTED DIPHOSPHONIC ACIDS AND ITS EFFECT ON METAL ION EXTRACTION

R. Chiarizia,[1] R. E. Barrans, Jr.,[1] J. R. Ferraro,[1] A. W. Herlinger,[2] and D. R. McAlister[2]

[1]Chemistry Division, Argonne National Laboratory*, Argonne, Illinois
[2]Chemistry Department, Loyola University Chicago, Chicago, Illinois

ABSTRACT

Solvent extraction reagents containing the diphosphonic acid group exhibit an extraordinary affinity for tri-, tetra-, and hexavalent actinides. Their use has been considered for actinide separation and preconcentration procedures. Solvent extraction data obtained with P,P′-di(2-ethylhexyl) methane-, ethane-, and butanediphosphonic acids exhibit features that are difficult to explain without knowl-

*The work at ANL was performed under the auspices of the Office of Basic Energy Sciences, Division of Chemical Sciences, U.S. Department of Energy, under contract W-31-109-ENG-38.

Published by Marcel Dekker, Inc. www.dekker.com

edge of the aggregation state of the extractants. Information about the aggregation of the dialkyl-substituted diphosphonic acids in aromatic diluents has been obtained using the complementary techniques of vapor pressure osmometry, small-angle neutron scattering, infrared spectroscopy, and molecular mechanics. The results from these techniques provide an understanding of the aggregation behavior of these extractants that is fully compatible with the solvent extraction data. The most important results and their relevance to solvent extraction are reviewed in this paper.

INTRODUCTION

Aqueous soluble diphosphonic acids are powerful complexing agents for a wide variety of metal ions, especially actinides and lanthanides (1,2). The chelating ion-exchange resin Diphonix® contains a geminally substituted diphosphonic acid ligand chemically bonded to a styrene-based polymeric matrix. Because of its extraordinarily strong affinity for actinide ions and for iron(III), the resin has found application in procedures for actinide separations and in hydrometallurgical processes where efficient separation of Fe(III) from other transition metals is required (3).

P,P′-di(alkyl) alkyldiphosphonic acids are the solvent extraction equivalent of the Diphonix resin. A general formula for some recently developed dialkyl-substituted diphosphonic acid solvent extraction reagents is shown in Structure 1:

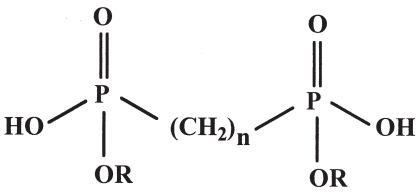

Structure 1.

where *R* is the 2-ethylhexyl group and *n* is one, two or four, for P,P′-di(2-ethylhexyl) methane- (H_2DEH[MDP]), ethane- (H_2DEH[EDP]), and butane- (H_2DEH[BuDP]) diphosphonic acids, respectively. The recently developed extraction chromatographic resin Dipex® is a noteworthy example of a practical application of H_2DEH[MDP] in actinide separation procedures (4).

It is well established that acidic organophosphorus extractants strongly aggregate in nonpolar diluents (5,6). Monoprotic acids usually dimerize to form an $R_2^2(8)$ ring, analogous to that formed in the familiar dimerization of carboxylic acids. $R_2^2(8)$, in the Etter hydrogen bond assembly classification (7), denotes an eight-membered ring structure containing two hydrogen bond donors and two hy-

drogen bond acceptors. Hydrogen bonding in organophosphorus acid dimers, however, is known to be stronger than in carboxylic acid dimers (8,9). The aggregation behavior of diprotic acids is more complicated. When two monomers hydrogen-bond to form a dimeric species containing one $R_2^2(8)$ ring, the resulting aggregate has additional -OH groups that can serve as sites for further aggregation (10). This explains why di(2-ethylhexyl) phosphoric acid, HDEHP, is dimeric in benzene (6,11), whereas the diprotic acid mono(2-ethylhexyl) phosphoric acid, H_2MEHP, can have an aggregation number as high as 12 in the same diluent (11,12).

Because HDEHP and H_2MEHP can be regarded as monofunctional analogues of the diphosphonic acids shown in Structure 1, the question arises as to whether the aggregation behaviors of H_2DEH[MDP], H_2DEH[EDP], and H_2DEH[BuDP] are similar to that of a dibasic acid or if aggregation is limited to the formation of dimers like a monobasic acid.

Knowledge of the aggregation state of an extractant is not only important from a basic structural point of view, but is also vital for understanding metal extraction chemistry—especially the interpretation of the slope values of extractant dependencies. In solvent extraction systems characterized by extensive extractant aggregation, extractant dependencies are generally unity and independent of the type of metal ion extracted. This type of behavior has been reported for the extraction of actinides and lanthanides by H_2MEHP in aromatic diluents (10,12,13). With highly aggregated extractants such as H_2MEHP, metal ions are buried within the extractant aggregate and held in place by forces analogous to those in solid ion-exchange resins (10). Similar results have been reported for other highly aggregated extractants, for example, quaternary alkylammonium salts (14) and dinonylnaphthalene sulfonic acid in nondepolymerizing diluents (15). These examples illustrate the effect that the aggregation state of the extractant molecule can have on the metal extraction chemistry.

The aggregation behavior of H_2DEH[MDP], H_2DEH[EDP], and H_2DEH[BuDP] in aromatic diluents has been investigated by infrared spectroscopy, vapor pressure osmometry (VPO), molecular mechanics methods, and small-angle neutron scattering (SANS). These complementary techniques have provided valuable insights into the unique metal solvent extraction data exhibited by these compounds. The objective of the present work is to summarize the results of our recent aggregation studies and to illustrate how these results provide an understanding of the metal solvent extraction chemistry.

EXPERIMENTAL METHODS

Materials

The preparation, purification, and properties of H_2DEH[MDP], H_2DEH[EDP], and H_2DEH[BuDP], as well as the radioisotopes and other reagents used in this work, have been described previously (16–18).

MARCEL DEKKER, INC.
270 Madison Avenue, New York, New York 10016

Techniques

The distribution ratio measurements were performed as reported (16–18). The diluent used for the distribution ratio experiments was *o*-xylene. Toluene was a more convenient diluent for the other measurements. The behavior of the extractants is not expected to change appreciably when toluene replaces *o*-xylene as the diluent. The details of the VPO and IR measurements can be found in the literature (18–23); those of the molecular mechanics calculations on H_2DEH[MDP] have also been reported (23). The VPO technique, similarly to other measurements of colligative properties, allows an estimation of the number of solute particles present in the test solution, from which the number average aggregation number (n) of the solute can be calculated.

The SANS technique is based on the large difference in the neutron scattering properties of the hydrogen and deuterium atoms. This difference is exploited in neutron structural studies of polymers, micellar aggregates, and other materials. Dissolution of an extractant in a deuterated diluent provides the neutron scattering contrast required to make the solute particles "visible" against the solvent background. SANS measurements of deuterated toluene solutions of H_2DEH[MDP], H_2DEH[EDP], H_2DEH[BuDP], and their metal complexes were made using the time-of-flight small-angle neutron diffractometers (SAD and SAND) at the Intense Pulsed Neutron Source (IPNS) at Argonne National Laboratory (24–26).

SAD and SAND use pulsed neutrons with wavelengths in the range 0.5–14 Å and fixed sample-to-detector distances of 1.5 m and 2.0 m, respectively. These instruments provide useful ranges of momentum transfer [$(Q = (4\pi/\lambda)\sin\Theta$, where Θ is half the scattering angle and λ is the wavelength of the probing neutrons] of 0.005–0.35 $Å^{-1}$ and 0.003–0.7 $Å^{-1}$, respectively. Other characteristics of the diffractometers have been reported in the literature (24–26). The reduced data for each sample were corrected for the backgrounds from the instrument, the quartz cell, and the solvent. The reduced data were then placed on an absolute scale by using a polymer melt sample containing an equal-volume mixture of deuterated and hydrogenous high-molecular-weight polystyrenes whose absolute cross section are known.

The SANS scattering signals were interpreted using the Guinier analysis $\{\ln[I(Q)]$ vs. $Q^2\}$ (27), where I is the scattering intensity and Q has been defined as given above. When the scattering patterns showed evidence of particle elongation, the modified-Guinier analysis for rodlike particles $\{\ln[I(Q)\sum Q]$ vs. $Q^2\}$ (28) was performed. The Guinier analysis of the data provides the radius of gyration, R_g. R_g is a measure of the spatial extension of the particle and is given by the root-mean-squared distance of all the atoms from the centroid of the scattering particle. For example, for a spherical particle with radius R, R_g can be obtained from $R_g = R\sqrt{(3/5)}$, whereas for a cylindrical particle with radius R and length L, R_g is given by $R_g = \sqrt{(R^2/2+L^2/12)}$. The modified-Guinier analysis for rodlike parti-

MARCEL DEKKER, INC.
270 Madison Avenue, New York, New York 10016

cles, on the other hand, allows an estimation of the cross-sectional radius of gyration, R_c, of the rodlike structure, where $R_c = \sqrt{(R^2/2)}$, from the slope of the straight line describing the $\{\ln[I(Q)\cdot Q]$ vs. $Q^2\}$ data.

Because the SANS data are available on an absolute scale, the Guinier fit can be used to determine the molecular weight of the extractant aggregates and, hence, the aggregation number. In the absence of interactions between scattering particles and at low particle concentration, the SANS intensity $I(Q)$ can be written as:

$$I(Q) = N_p\,(\rho_p - \rho_s)^2\,V_p^2\,P(Q)\text{-}, \tag{1}$$

where $P(Q)$ is the single-particle form factor describing the angular distribution of the scattering as a function of size and shape of the particle (29), N_p and V_p are the number of scattering particles per unit volume and the volume of the particle, and ρ_p and ρ_s are the scattering length densities of the solute and the deuterated toluene, respectively. Because $P(Q) = 1$ when $Q = 0$, the extrapolated scattering intensity at 0^o, $I_{(0)}$, derived from the y-axis intercept of the Guinier fit, can be written as

$$I_{(0)} = N_p\,(\rho_p - \rho_s)^2\,V_p^2 \tag{2}$$

After substitutions and rearrangement, Equation (2) was used to calculate the weight-average molecular weights of the aggregates from which the weight-average aggregation numbers (n_w) of the extractants were obtained.

Equation (1) can also be used to gain information about the shape of the solute particles, as form factors have been calculated for many different particle shapes (30). The equation of the form factor $P(Q,R)$ for a homogeneous sphere of radius R was used to fit the scattering data of H_2DEH[EDP] (26).

RESULTS AND DISCUSSION

Solvent Extraction Data

Distribution data have been obtained for the extraction of alkaline earth cations (Ca^{2+}, Sr^{2+}, Ba^{2+}, and Ra^{2+}), Fe(III), and representative tri-, tetra-, and hexavalent actinide ions [Am(III), Th(IV), and U(VI)] by *o*-xylene solutions of H_2DEH[MDP], H_2DEH[EDP], and H_2DEH[BuDP]. For each metal ion–extractant system, acid and extractant dependencies have been determined. A complete account of the extraction data can be found in references 16–18. Some representative data, however, will be presented here.

Figure 1 summarizes the extractant dependencies measured for the extraction of Am(III) by H_2DEH[MDP], H_2DEH[EDP], and H_2DEH[BuDP] in *o*-xylene. Similar results were obtained for alkaline earth cations and U(VI) (16–18). The data of Figure 1 show that the slope values of the extractant dependencies

MARCEL DEKKER, INC.
270 Madison Avenue, New York, New York 10016

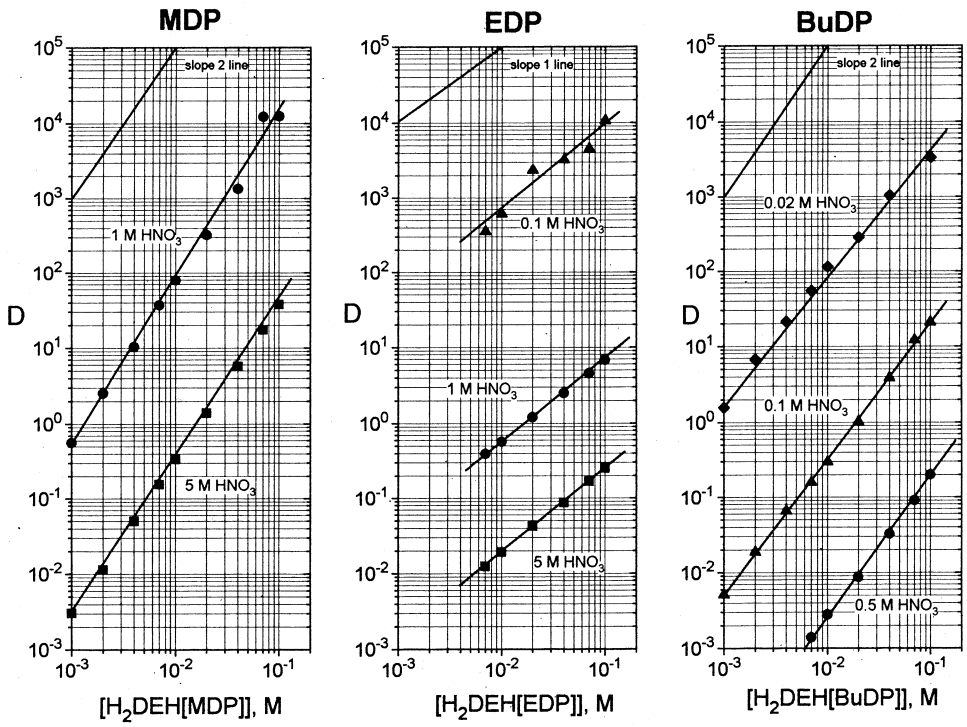

Figure 1. Distribution ratio, *D*, vs initial extractant concentration in the extraction of Am(III) by H_2DEH[MDP], H_2DEH[EDP], and H_2DEH[BuDP] in *o*-xylene from aqueous solutions containing different concentrations of HNO_3.

measured for H_2DEH[MDP] and H_2DEH[BuDP] are equal to 2, whereas those measured for H_2DEH[EDP] are equal to 1. Based on the arguments presented earlier, this behavior led us to suspect that H_2DEH[MDP] and H_2DEH[BuDP] form small aggregates in *o*-xylene, whereas H_2DEH[EDP] may form much larger aggregates. To obtain a quantitative estimate of the extractant aggregation, however, different types of measurements were needed.

Infrared Spectroscopy

Infrared spectra of 0.15 M toluene solutions of H_2DEH[MDP], H_2DEH[EDP], and H_2DEH[BuDP] are shown in Figure 2. A complete discussion of these spectra and their changes on metal extraction has been given (18–23).

MARCEL DEKKER, INC.
270 Madison Avenue, New York, New York 10016

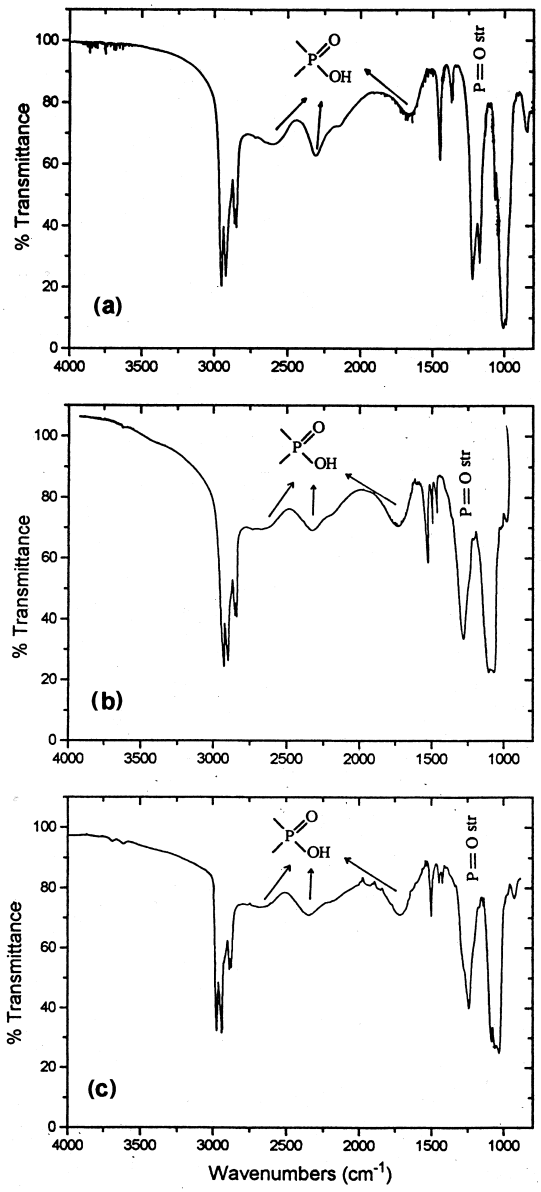

Figure 2. Infrared spectra of 0.15 M toluene solutions of (a) H_2DEH[MDP], (b) H_2DEH[EDP], and (c) H_2DEH[BuDP].

MARCEL DEKKER, INC.
270 Madison Avenue, New York, New York 10016

Only spectral features that are directly related to extractant aggregation are discussed in the present study.

None of the absorption bands in the spectra shown in Figure 2 can be attributed to free hydroxyl groups. Three broad bands of medium intensity, characteristic of the P(O)(OH) group of an alkyl phosphonic acid, appear at relatively low frequencies at about 2700, 2300, and 1700 cm^{-1}. This behavior is characteristic of O-H groups that are strongly involved in hydrogen bonding to phosphoryl oxygen atoms (11,12). These three bands disappear on metal salt formation, as expected.

Some of the strongest absorption bands in the spectra occur in the 950–1250 cm^{-1} region. The band at ~1200 cm^{-1} is of particular interest. It has been assigned as a phosphoryl absorption band by comparison with the spectra of related organophosphorus acids (31,32). The frequency of this band is considerably lower than that reported for the corresponding tetraethyl esters due to strong hydrogen bonding with the P-OH group (33). These spectral features, characteristic of systems with strong intermolecular hydrogen bonding, clearly indicate that H_2DEH[MDP], H_2DEH[EDP], and H_2DEH[BuDP] exist in solutions as aggregates. Strong hydrogen bonding is, in fact, the key to the stability of the aggregates. No quantitative information on the type of aggregates (i.e., dimers vs. higher aggregates), however, is provided by the infrared spectra.

A striking feature of the H_2DEH[MDP] spectrum is the P=O band splitting. For H_2DEH[EDP] and H_2DEH[BuDP], a single broad P=O stretching band is observed. The appearance of two bands in the P=O stretching region of the spectrum of H_2DEH[MDP] initially led to the hypothesis that two different types of hydrogen bonds (i.e., intra- and intermolecular) were present in the aggregate. The appearance of a single phosphoryl band in the spectra of H_2DEH[EDP] and H_2DEH[BuDP] implies that all the hydrogen bonds in the aggregate are equivalent.

Infrared spectra spectra of toluene solutions of H_2DEH[MDP], H_2DEH[EDP], and H_2DEH[BuDP] after metal extraction from aqueous solutions in some cases showed water absorption bands at ~3400 and ~1660 cm^{-1}. This indicates that with some metal ions, water as well as the metal ions are extracted by the diphosphonic acids. Although no quantitative study of water extraction was performed, the water absorption bands were particularly strong in the extraction of alkaline earth cations and Eu(III) by H_2DEH[EDP]. H_2DEH[EDP] is unique in its ability to extract water. In fact, even solutions of H_2DEH[EDP] preequilibrated with aqueous nitric acid in the absence of metal ions exhibit characteristic water absorption bands. Coextraction of water is generally observed when the extractant forms large aggregates in the organic phase that behave like reverse micelles (34,35).

MARCEL DEKKER, INC.
270 Madison Avenue, New York, New York 10016

Osmometric Measurements

VPO measurements of toluene solutions of H_2DEH[MDP], H_2DEH[EDP], and H_2DEH[BuDP] were used to determine aggregation numbers for these in a nonpolar diluent (18–20). Some typical results are compared in Figure 3 with data for the monomeric standard bibenzyl. To a first approximation, the VPO plots are linear in the concentration range investigated. Thus, the aggregation number (n) of an extractant can be obtained simply from the ratio of the slope of the standard to that of the extractant. The data in Figure 3 clearly indicate that H_2DEH[MDP] forms dimeric species, whereas H_2DEH[EDP] and H_2DEH[BuDP] form hexameric and trimeric aggregates, respectively.

Complementary VPO measurements were made of solutions of the extractants after loading the organic phase with selected metal ions through solvent extraction. The data revealed that in several cases, at high metal concentrations

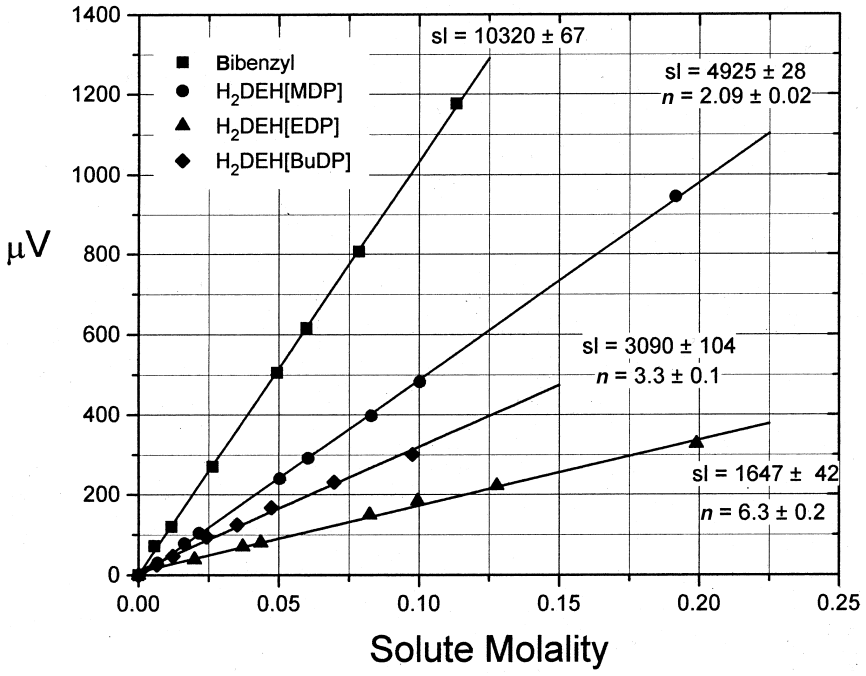

Figure 3. Osmometric measurements with H_2DEH[MDP], H_2DEH[EDP], and H_2DEH[BuDP] in toluene at T = 25°C. Standard = bibenzyl; slope values of the lines and aggregation numbers (n) are shown in the figure.

MARCEL DEKKER, INC.
270 Madison Avenue, New York, New York 10016

in the organic phase, the metal-extractant complexes were highly aggregated. This was particularly evident for the Fe(III)-H_2DEH[MDP] and the Fe(III)-H_2DEH[BuDP] systems, for which average aggregation numbers as high as ~33 and ~18, respectively, were obtained (18,19). With H_2DEH[EDP], the average aggregation number remained essentially unchanged after extraction of metal ions at high concentration (20). This implies that in many cases the hexameric aggregation of the extractant is not disrupted by the extraction of metal ions. This result reaffirms the unique solvent extraction behavior of H_2DEH[EDP].

The highly aggregated state of H_2DEH[EDP], which is not disrupted by metal extraction, explains the extractant dependencies reported in Figure 1. Assuming that the hexameric aggregates of H_2DEH[EDP] behave as reverse micelles in solution, cations could be transferred into the hydrophilic cavity of the aggregate without disrupting aggregation while retaining most of their hydration sphere. This view is consistent with the strong water absorption bands observed in the infrared measurements for H_2DEH[EDP].

Based on this extraction mechanism, it was possible to calculate the value of the aggregation constant for H_2DEH[EDP] from the alkaline earth extractant dependency data (17), following an approach similar to that used previously to explain analogous effects in metal ion extraction by dialkylnaphthalene sulfonic acids (34,36). Following this procedure, a β_6 value of $(6 \pm 1) \times 10^{13}$ was obtained.

The aggregation constants for H_2DEH[BuDP] were obtained from osmometric measurements (18). The VPO data for H_2DEH[BuDP] reported in Figure 3 show a small deviation from linearity. The straight-line fit of the data has a slope consistent with an average aggregation number of about 3.3. This strongly suggests the formation of predominantly trimeric aggregates in equilibrium with other somewhat larger species. By best-fitting the data with mass balance and aggregation equilibria expressions, it was found that the aggregation of H_2DEH[BuDP] in toluene is most accurately described as an equilibrium involving the formation of trimeric and hexameric species with $\beta_3 = (6.2 \pm 1.6) \times 10^6$ and $\beta_6 = (1.8 \pm 0.5) \times 10^{14}$. Using these β values, it is easy to show that the trimer is the predominant H_2DEH[BuDP] species present in solution at concentrations up to 0.1 M. This aggregate is assumed to be the primary metal-extracting species.

Figure 1 clearly shows that the solvent extraction behavior of H_2DEH[BuDP] is different from that of H_2DEH[EDP]. It is interesting to note that both the H_2DEH[BuDP] trimer and the H_2DEH[EDP] hexamer contain a total of 12 carbon atoms in the alkyl chains separating the phosphorus atoms. The two aggregates, however, should be different. The internal core of the H_2DEH[BuDP] aggregate should be considerably less hydrophilic than the interior of the H_2DEH[EDP] hexamer because of the smaller number of polar P(O)(OH) groups.

MARCEL DEKKER, INC.
270 Madison Avenue, New York, New York 10016

As a result, the solvent extraction of metal ions by a H_2DEH[BuDP] trimer is expected to be quite different from that of the H_2DEH[EDP] hexamer.

In the case of the H_2DEH[MDP] dimer, it was not possible to calculate the dimerization constant. The linearity of the VPO data shown in Figure 3 indicates that the dimerization constant is sufficiently large that the ligand is dimeric over the entire concentration range investigated.

Conformation of the H_2DEH[MDP] Dimer

Possible structures for the H_2DEH[MDP] dimer are shown in 2–5 below:

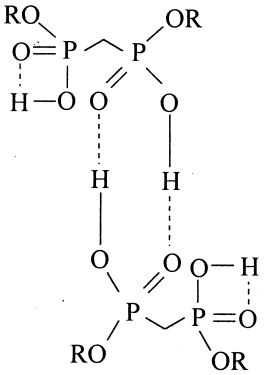

Structure 2.

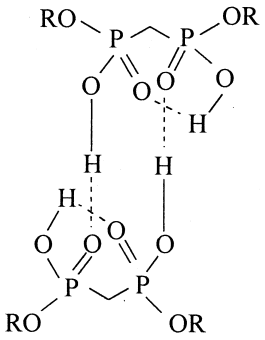

Structure 3.

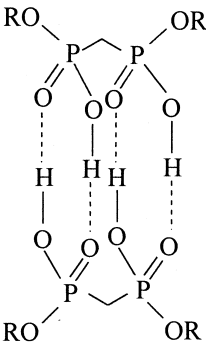

Structure 4.

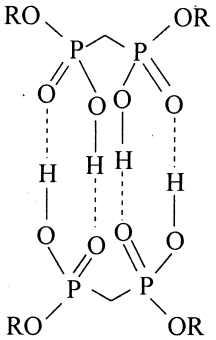

Structure 5.

MARCEL DEKKER, INC.
270 Madison Avenue, New York, New York 10016

As mentioned earlier, the appearance of two bands in the phosphoryl stretching region of the infrared spectrum of H_2DEH[MDP] suggested that the dimer might contain two different types of hydrogen bonds, as shown in Structure 2 or 3 (the symmetrical conformations 4 and 5 only contain intermolecular hydrogen bonds). This possibility was tested by continuous-variation infrared spectroscopic studies. In these investigations, the effect on the P=O stretching vibration of progressively replacing the CCl_4 diluent in a solution of H_2DEH[MDP] with the depolymerizing diluent 1-decanol was measured (23). [Note that the spectra of the diphosphonic acids in CCl_4 and toluene are identical, so that the following considerations apply to both diluents (23)].

The intramolecular hydrogen bonds in the $R_1^1(4)$ and $R_1^1(6)$ moieties of Structures 2 and 3, respectively, are expected to be disrupted by added decanol sooner than the intermolecular hydrogen-bonded rings. Thus, the band corresponding to the $R_1^1(4)$ or $R_1^1(6)$ moieties should shift gradually as decanol is added. In dimer Structures 4 and 5, which contain two adjacent $R_2^2(8)$ moieties, the entire structure would be destabilized by replacement of any one of the four hydrogen bonds by hydrogen bonds to decanol. The single P=O stretching band anticipated for these structures would be expected to abruptly shift at the decanol concentration at which the dimer dissociates.

The observed infrared spectra of H_2DEH[MDP] in the presence of increasing concentrations of decanol showed that one absorption in the P=O stretching region (1189 cm^{-1}) remained constant even when the CCl_4 solvent was entirely replaced by decanol. The other absorption band in this region remained constant at 1238 cm^{-1} as the solvent was changed incrementally from CCl_4 to a CCl_4-decanol mixture where the decanol concentration was eight times the concentration of the diphosphonic acid. Upon complete replacement of the solvent by decanol, this band shifted abruptly to 1231 cm^{-1}.

Because the 1189-cm^{-1} band is solvent independently and still present when the diphosphonic acids are monomeric, it cannot be reasonably assigned to a hydrogen-bonded P=O stretching mode. This band must arise from another mode that coincidentally occurs in this region (23). The 1238-cm^{-1} band of H_2DEH[MDP], therefore, is assigned as the only P=O stretching vibration. The abrupt shift of this band upon complete solvent replacement is consistent with Structures 4 and 5.

To fully elucidate the relative stabilities of structures III-VI, molecular mechanics calculations were performed. A variety of starting structures containing two (such as 2 and 3) or four (such as 4 and 5) intermolecular hydrogen bonds were generated and geometrically optimized. For ease of computation, the 2-ethylhexyl groups in H_2DEH[MDP] were replaced by methyl groups. Two highly hydrogen-bonded dimer structures were found to be the most stable. They exhibited the hydrogen-bonding patterns of Structures 4 or 5. The lowest energy conformation found for Structure 5 was slightly higher in energy than the lowest en-

MARCEL DEKKER, INC.
270 Madison Avenue, New York, New York 10016

ergy conformation found for Structure 4. The hydrogen bonding in 5 is expected to be slightly weaker than in 4, due to larger intermolecular H···H repulsions, as illustrated following:

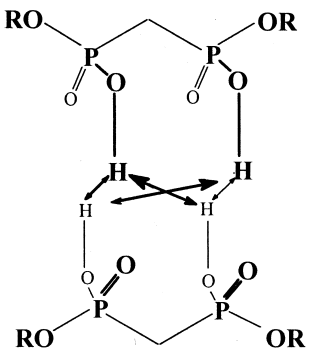

Structure 6.

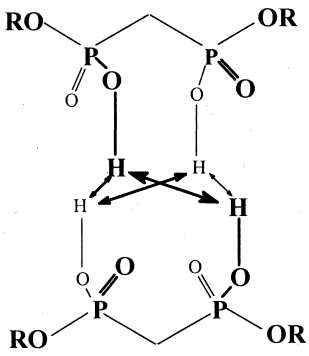

Structure 7.

In these structures, the intermolecular proton-proton repulsions in dimer Structures 6 and 7 are represented as arrows. Repulsions are both within $R_2^2(8)$ rings and between adjacent rings. In Structure 6, the intermolecular interring repulsions are between protons at opposite corners of the dimer; in Structure 7, they are between protons at adjacent corners. The calculated energy difference is less than 1 kcal/mol, which suggests that both 6 and 7 are populated in an equilibrium mixture (23).

SANS Investigations

SANS is a powerful technique in the structural studies of polymers and micelles (37). Recent studies have shown the applicability of this technique to solvent extraction chemistry. SANS has the unique ability to elucidate the size and shape of both the extractant aggregates and the polymeric species formed on metal ion extraction (38–41). The need exists for a better knowledge of the species that are formed under conditions likely to be met in practical applications of solvent extraction (i.e., at high metal loading of the organic phase). Under these conditions, large aggregates or polymeric species are often formed that have not been studied in detail (35). The application of SANS to this aspect of solvent extraction chemistry is particularly promising.

SANS studies of the aggregation of H_2DEH[MDP], H_2DEH[EDP], and H_2DEH[BuDP] dissolved in deuterated toluene have been performed (24–26). The results of these studies, summarized in Table 1, substantiate the VPO results

MARCEL DEKKER, INC.
270 Madison Avenue, New York, New York 10016

discussed earlier. The R_g values clearly indicate that the H_2DEH[EDP] and H_2DEH[BuDP] aggregates are significantly larger than the H_2DEH[MDP] aggregate. More specifically, the n_w values of Table 1 confirm that H_2DEH[MDP] exists in solution as a dimer, H_2DEH[EDP] as a hexamer, and H_2DEH[BuDP] predominantly as a trimer. The n_w value obtained for a 0.05 M solution of H_2DEH[BuDP] is slightly lower than that obtained for a 0.1 M solution. This result is consistent with our earlier observations, which suggested a low concentration of hexameric aggregates in equilibrium with a higher concentration of H_2DEH[BuDP] trimers (18).

In our attempts to obtain more detailed information about the three-dimensional shape of the H_2DEH[EDP] aggregate, we were able to fit the SANS data using the equation of the form factor for a homogeneous sphere (30). The very good fit, shown in Figure 4, provided a radius R of the spherical aggregate equal to 11.8 ± 0.2 Å. In this aggregate, the alkyl groups are likely oriented outward (toward the solvent), and a large hydrophilic internal cavity is available to accommodate metal cations and/or water molecules.

Because the VPO data discussed earlier revealed the tendency of some metal-extractant complexes to aggregate extensively in the organic phase, SANS measurements were also performed on deuterated toluene solutions of the three diphosphonic acids after extraction of progressively higher concentrations of selected metal cations (24–26).

The SANS data revealed that both U(7) and Th(3) form large aggregates with H_2DEH[MDP]. This is particularly true for Th(3), for which aggregates containing up to ~200 ligand molecules were identified (25). These aggregates grow in three dimensions, and it is likely that these species have the same three-dimensional structure as the Th(DEH[MDP])$_2$ salt that precipitates under very high metal loading conditions in the biphasic system used to extract Th(IV).

The Fe(III)-H_2DEH[MDP] system is particularly striking. The SANS results confirmed the tendency of the Fe(III) complexes with H_2DEH[MDP] to ag-

Table 1. Radius of Gyration, R_g, and Aggregation Number, n_w, for Di(2-ethylhexyl)-Substituted Diphosphonic Acids in Deuterated Toluene

Acid	Molarity (M)	R_g (Å)	n_w
H_2DEH[MDP]	0.10	6.9 ± 0.5	2.1 ± 0.1
H_2DEH[EDP]	0.05	10.1 ± 0.5	5.7 ± 0.5
H_2DEH[EDP]	0.10	10.6 ± 0.6	5.8 ± 0.5
H_2DEH[BuDP]	0.05	7.4 ± 1.3	2.9 ± 0.2
H_2DEH[BuDP]	0.10	12.4 ± 0.3	3.6 ± 0.3

MARCEL DEKKER, INC.
270 Madison Avenue, New York, New York 10016

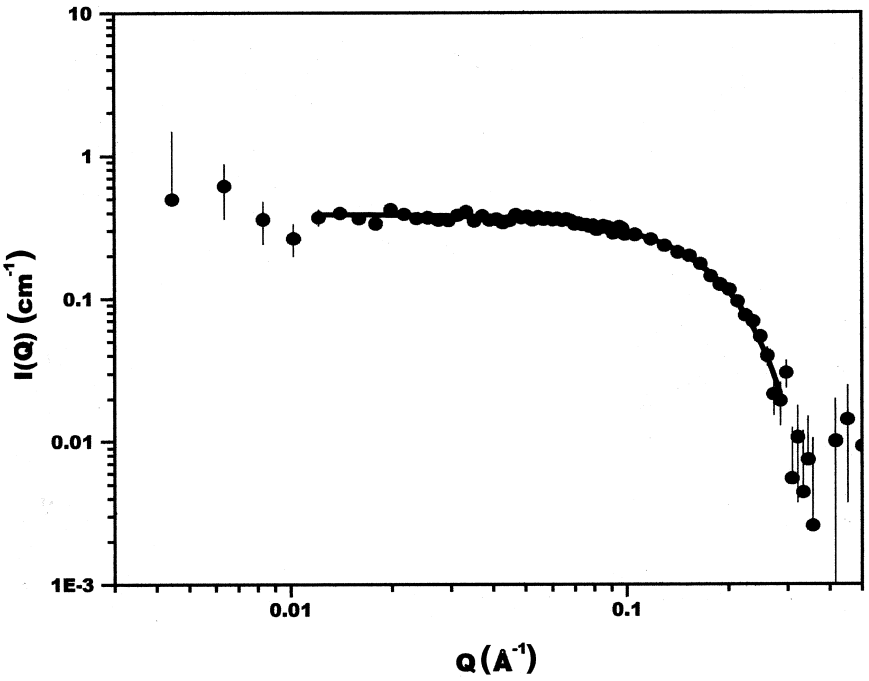

Figure 4. Fit of the SANS data for 0.1 M H_2DEH[EDP] in deuterated toluene with the equation of the form factor for a homogeneous sphere with a radius $R = 11.8 \pm 0.2$ Å. $I(Q)$ is the scattering intensity, and Q is the momentum transfer, $(4\pi/\lambda)\sin\Theta$, where Θ is half the scattering angle and λ is the wavelength of the neutrons.

gregate extensively. Further, the measurements revealed the presence of rodlike particles of constant radius but variable length, which depends on the concentration of metal in the organic phase. As more metal is brought into the organic phase, particle growth is propagated by attachment to terminal sites of the existing rodlike aggregates. Table 2 reports the radius of gyration, aggregation number, and radius and length of the rodlike particles identified after extraction of Fe(III) from aqueous solutions containing different HNO_3 concentrations.

The average radius of 9 Å for the aggregates reported in Table 2 agrees with results of previous SANS investigations on monofunctional analogues of H_2DEH[MDP] (38). It is reasonable to assume that the hydrocarbon chains of the ester are oriented toward the exterior of the cylindrical aggregates, whereas the metal ions interact with the polar groups of the extractant, which are oriented toward the interior of the cylinder. Thus, the metal ions are located along a channel

Table 2. Gyration Radius (R_g), Aggregation Number (n_w), Radius (R), and Length (L) for Rod-Shaped Aggregates Formed in the Extraction of Fe(III) by 0.1 M H_2DEH[MDP]

$[Fe]_{og}$ (M)	$[H_2DEH[MDP]]/[Fe]_{org}$	R_g (Å)	n_w	R (Å)	L (Å)
0.00972[a]	10.29	7.4 ± 0.3	2.8 ± 0.04		
0.0252[a]	3.96	8.3 ± 0.3	4.6 ± 0.05		
0.0447[a]	2.24	20 ± 0.7	17 ± 0.2	8.8 ± 0.4	66
0.0586[a]	1.71	70 ± 7.9	70 ± 4	10.2 ± 0.5	241
0.0248[b]	4.03	8.4 ± 0.4	4.2 ± 0.07		
0.0413[b]	2.42	17 ± 1.1	12 ± 0.3	8.9 ± 0.6	55
0.0540[b]	1.85	30 ± 1.8	21 ± 2	8.9 ± 0.6	102
0.0589[b]	1.70	88 ± 30	110 ± 22	7.6 ± 0.1	304
0.0240[c]	4.17	7.7 ± 0.4	4.1 ± 0.07		
0.0463[c]	2.16	35 ± 3.3	23 ± 0.8	8.9 ± 0.4	119
0.0551[c]	1.81	48 ± 3.7	36 ± 4	8.9 ± 0.5	165
0.0476[c]	2.18	80 ± 7.9	69 ± 5	10.2 ± 0.2	276

[a] Fe(III) extracted from 0.1 M HNO_3.
[b] Fe(III) extracted from 1 M HNO_3.
[c] Fe(III) extracted from 5 M HNO_3.

in the center of the cylinder. If this is the case, a plausible structure of the metal-extractant polymeric species is shown in Structure 8:

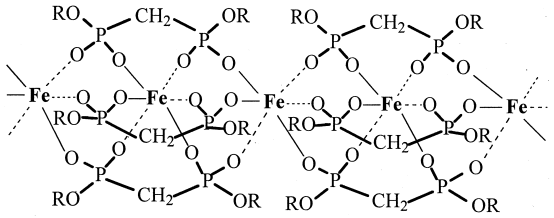

Structure 8.

Similar structures have been recently observed for solid-state and eight- and seven-coordinate crystalline lanthanide complexes of 1-hydroxyethane-1,1-diphosphonic acid, HEDPA (an aqueous-soluble, non-alkyl-substituted analogue of H_2DEH[MDP]) (42).

Assuming a structure of this type for the Fe(III)-H_2DEH[MDP] aggregates, the SANS data have been used to calculate the distance between neighboring Fe(III) atoms in the chain (24). The Fe-Fe distance in the Fe(III)-

MARCEL DEKKER, INC.
270 Madison Avenue, New York, New York 10016

H_2DEH[MDP] aggregates was calculated to be 3.7 ± 0.3 Å. This value is reasonable in view of the 4.7- to 5.8-Å metal-metal distances found in lanthanide HEDPA complexes (42). Structure 8 and the 3.7-Å value of the Fe-Fe distance suggest the formation of covalent bonds between Fe(III) and the ligand molecules. Covalent binding of Fe(III) to H_2DEH[MDP] has been experimentally confirmed in a far-infrared investigation of the sodium, selected lanthanide, and Fe(III) salts of H_2DEH[MDP] (21). The Fe(III)-H_2DEH[MDP] salt exhibited a strong absorption band at 256 cm^{-1} that was not present in the spectrum of H_2DEH[MDP] or any of the other salts investigated. This band was assigned as a metal-oxygen stretching mode ($\nu_{M\text{-}OP}$), and the assignment was confirmed by the metal isotope technique, that is, by repeating the measurements on the ^{54}Fe-labeled complex. The 256-cm^{-1} absorption band shifted to higher frequency on substitution of the natural iron isotopic mixture (91.5% ^{56}Fe) with the lighter isotope. Only vibrations involving the motion of the metal atom are shifted by metal isotope substitution. The appearance of an isotope-sensitive metal-oxygen stretching band in the anhydrous Fe(III)-H_2DEH[MDP] complex indicates that the iron-diphosphonate interaction has a substantial covalent component.

Surprisingly, the SANS data did not indicate formation of large aggregates for the extraction of Fe(III) by H_2DEH[EDP] (26). The highest aggregation number for the Fe(III)-H_2DEH[EDP] complex was ~8. Apparently, the increase in the length of the alkyl bridge connecting the two P atoms of the ligand by one CH_2 group has a profound effect not only on the state of aggregation of the extractant itself, but also on the tendency of metal complexes to extensively aggregate.

The n_w values measured for H_2DEH[EDP] solutions after extraction of Ca(II), La(III), and U(VI) were not significantly different from the value for the extractant alone. In these cases, the aggregation number was ~6 (26). It was mentioned earlier that the extraction of some cations does not alter the infrared spectrum of the extractant and that water is coextracted. Thus, the SANS results confirmed that metal extraction occurs primarily through cation transfer into the hydrophilic cavity of the hexameric aggregate with little, if any, disruption of the solution structure of the extractant. This type of extraction, reminiscent of metal extraction by reverse micelles, is consistent with the extractant dependencies measured for alkaline earth cations, Am(III), and U(VI) (see, for example, Fig. 1). The SANS data obtained for a U(VI)-H_2DEH[EDP] solution with a ligand/metal ratio of ~2 were fitted with the form factor equation for a homogeneous sphere with a radius of 12.4 ± 0.5 Å (26). If the reverse micelle analogy applies to this solution as well, the n_w value of ~6 implies that three uranyl ions are present in the internal cavity of the hexameric aggregate. Thus, the spherical hexameric aggregate of H_2DEH[EDP] does not change its structure even at the maximum U(VI) loading attainable.

MARCEL DEKKER, INC.
270 Madison Avenue, New York, New York 10016

Large aggregates were also identified in solutions containing Fe(III)-H_2DEH[BuDP] complexes (26). As with the Fe(III)-H_2DEH[MDP] particles, these aggregates are rod-shaped. There is, however, a difference between the two systems. The Fe(III)-H_2DEH[MDP] aggregates have a constant radius and grow lengthwise with increasing Fe(III) concentration (24). In contrast, the Fe(III)-H_2DEH[BuDP] aggregates have an approximately constant length and a radius that increases with the Fe(III) concentration in the organic phase. It is likely that growth of the rodlike Fe(III)-H_2DEH[BuDP] aggregates occurs along the axis of the rod, as shown in Structure 9:

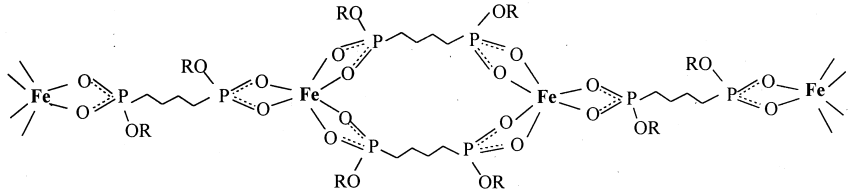

Structure 9.

In these aggregates, each Fe(III) atom only interacts with phosphonate groups belonging to different ligand molecules. In H_2DEH[BuDP], the donor atoms of the ligand are too far apart to interact simultaneously with the same metal atom. Solvent extraction studies have shown that H_2DEH[BuDP] interacts with metal ions in a way that is similar to its monofunctional analogues. The phosphonate groups of the ligand act independently of one another and complex metal ions in a noncooperative manner (18). With increasing metal concentration, the initially formed rodlike particles grow thicker. This growth presumably occurs via the opening of the ring formed by two ligand molecules bound to adjacent Fe(III) atoms (see Structure 9). Two sidearms that grow independently in a three-dimensional network are formed as a result.

CONCLUSIONS

The aggregation of the solvent extraction reagents P,P′-di(2-ethylhexyl) methane-, ethane-, and butanediphosphonic acids (H_2DEH[MDP], H_2DEH[EDP], and H_2DEH[BuDP], respectively) in toluene solutions has been investigated using the complementary techniques of infrared spectroscopy, VPO, molecular mechanics, and SANS.

The results of our investigations have shown that the length of the alkyl chain separating the two P atoms of the extractant molecule has a profound effect on the aggregation state of the extractant. The extractant aggregation state, in turn, strongly affects the metal solvent extraction chemistry.

MARCEL DEKKER, INC.
270 Madison Avenue, New York, New York 10016

Experimental and computational evidence has established that H_2DEH[MDP] is a dimer in toluene. The aggregate is stabilized by strong hydrogen bonding. The most stable conformation of the dimer is a closed, symmetrical structure containing only intermolecular hydrogen bonds with two adjacent $R_2^2(8)$ rings and a larger $R_2^2(12)$ moiety, such as Structures 6 and 7.

H_2DEH[EDP] forms hexameric, spherical aggregates in toluene. The hexameric H_2DEH[EDP] aggregates most likely adopt a structure comparable to that of reverse micelles. In these aggregates, the alkyl groups are oriented toward the solvent and a large hydrophilic internal cavity is available to accommodate metal cations. The highly aggregated state of H_2DEH[EDP] and the fact that the aggregation is not disrupted by the extraction of several metal cations have been used to explain the extractant dependencies of unity measured for the extraction of alkaline earth cations, Am(III) and U(VI). These metal ions are transferred into the hydrophilic cavity of the aggregate without disrupting its structure while retaining most, or part, of their hydration spheres.

The aggregation of H_2DEH[BuDP] in toluene is best described as an equilibrium involving the formation of trimeric and hexameric species. The trimer is the predominant species in the concentration range investigated. The internal core of the H_2DEH[BuDP] aggregate is less hydrophilic than that of the H_2DEH[EDP] hexamer because of the smaller number of polar P(O)(OH) groups. Consequently, the H_2DEH[BuDP] aggregates do not behave as reverse micelles in metal solvent extraction.

SANS investigations have demonstrated that large aggregates form when solutions of H_2DEH[MDP] and H_2DEH[BuDP] are used to extract certain metal ions under high metal-loading conditions. The largest aggregates have been observed in the extraction of Fe(III) and Th(IV). The Fe(III)-H_2DEH[MDP] aggregates are rods of constant radius whose length increases with the metal concentration in the organic phase. The Th(IV)-H_2DEH[MDP] and Fe(III)-H_2DEH[BuDP] aggregates are cylindrical, but growth also occurs laterally as more metal is transferred into the organic phase.

The formation of large aggregates has important implications for practical application of solvent extraction reagents. For example, if the extraction chromatographic resin Dipex, which contains H_2DEH[MDP] adsorbed in the pores of an inert support (4), is used to separate metal ions such as Fe(III) and actinides from solutions where the metal concentrations are relatively high, aggregated species may form. Because of their higher viscosities, these species might retard, or even prevent, further metal uptake. Stripping of the sorbed metal species from the resin, under these conditions, could also become difficult. Similar complications could arise in more conventional liquid-liquid solvent extraction procedures due to the formation of polymeric interfacial cruds even at relatively low metal loading of the organic phase.

MARCEL DEKKER, INC.
270 Madison Avenue, New York, New York 10016

ACKNOWLEDGMENTS

The work performed at ANL was funded by the U.S. Department of Energy, Office of Basic Energy Sciences, Division of Chemical Sciences, under contract W-31-109-ENG-38.

The authors wish to thank Ken Nash (ANL Chemistry Division) for useful discussions and advice and Volker Urban and Pappanan Thiyagarajan (ANL, IPNS) for introducing them to the small-angle neutron scattering technique.

REFERENCES

1. Rizkalla, E.N. Rev. Inorg. Chem. **1983,** *5*, 223.
2. Nash, K.L. Radiochim. Acta **1991,** *54*, 178.
3. Chiarizia, R.; Horwitz, E.P.; Alexandratos, S.D.; Gula, M.J. Sep. Sci. Technol. **1997,** *32*, 1 (and references therein).
4. Horwitz, E.P.; Chiarizia, R.; Dietz, M.L. React. Funct. Polym. **1997,** *33*, 25; U.S. Patent 5,651,883, issued July 29, 1997.
5. Marcus, Y.; Kertes, A.S. *Ion Exchange and Solvent Extraction of Metal Complexes*; John Wiley & Sons, Ltd.: New York, 1969.
6. Kolarik, Z. Solvent Extr. Rev. **1971,** *1*, 1.
7. Etter, M.C. Acc. Chem. Res. ***1990,*** *23*, 120.
8. Peppard, D.F.; Ferraro, J.R.; Mason, G.W. J. Inorg. Nucl. Chem. **1959,** *12*, 60.
9. Peppard, D.F.; Ferraro, J.R.; Mason, G.W. J. Inorg. Nucl. Chem. **1958,** *7*, 231.
10. Peppard, D.F.; Mason, G.W.; Driscoll, W.J.; Sironen, R.J. J. Inorg. Nucl. Chem. **1958,** *7*, 276.
11. Ferraro, J.R.; Mason, G.W.; Peppard, D.F. J. Inorg. Nucl. Chem. **1961,** *22*, 285.
12. Rao, G.S.; Mason, G.W.; Peppard, D.F. J. Inorg. Nucl. Chem. **1966,** *28*, 887.
13. Mason, G.W.; McCarty, S.; Peppard, D.F. J. Inorg. Nucl. Chem. **1962,** *24*, 967.
14. Chiarizia, R.; Gatrone, R.C.; Horwitz, E.P. Solvent Extr. Ion Exch. **1995,** *13*, 65.
15. Högfeldt, E.; Chiarizia, R.; Danesi, P.R.; Soldatov, V.S. Chem. Scri. **1981,** *18*, 13.
16. Chiarizia, R.; Horwitz, E.P.; Rickert, P.G.; Herlinger, A.W. Solvent Extr. Ion Exch. **1996,** *14*, 773.
17. Chiarizia, R.; Herlinger, A.W.; Horwitz, E.P. Solvent Extr. Ion Exch. **1997,** *15*, 417.

MARCEL DEKKER, INC.
270 Madison Avenue, New York, New York 10016

18. Chiarizia, R.; Herlinger, A.W.; Cheng, Y.D.; Ferraro, J.R.; Rickert, P.G.; Horwitz, E.P. Solvent Extr. Ion Exch. **1998,** *16*, 505.
19. Herlinger, A.W.; Chiarizia, R.; Ferraro, J.R.; Horwitz, E.P. Polyhedron **1997,** *16*, 1843.
20. Herlinger, A.W.; Chiarizia, R.; Ferraro, J.R.; Rickert, P.G.; Horwitz, E.P. Solvent Extr. Ion Exch. **1997,** *15*, 401.
21. Herlinger, A.W.; Ferraro, J.R.; Garcia, J.A.; Chiarizia, R. *Polyhedron* **1998,** *17*, 1471.
22. Ferraro, J.R.; Herlinger, A.W.; Chiarizia, R. Solvent Extr. Ion Exch. **1998,** *16*, 775.
23. Barrans Jr., R.E.; McAlister, D.R.; Herlinger, A.W.; Chiarizia, R.; Ferraro, J.R. Solvent Extr. Ion Exch. **1999,** *17*, 1195.
24. Chiarizia, R.; Urban, V.; Thiyagarajan, P.; Herlinger, A.W. Solvent Extr. Ion Exch. **1998,** *16*, 1257.
25. Chiarizia, R.; Urban, V.; Thiyagarajan, P.; Herlinger, A.W. Solvent Extr. Ion Exch. **1999,** *17*, 113.
26. Chiarizia, R.; Urban, V.; Thiyagarajan, P.; Herlinger, A.W. Solvent Extr. Ion Exch. **1999,** *17*, 1171.
27. Guinier, A.; Fournet, G. *Small Angle Scattering of X-Rays*; John Wiley and Sons: New York, 1955.
28. Porod, G. In *Small Angle X-Ray Scattering*; Glatter, O., Kratky, O., Eds., Academic Press: New York, 1982; Chap. 2.
29. Chen, S.H. Ann. Rev. Phys. Chem. **1986,** *37*, 351.
30. Pedersen, J.S. Adv. Colloid Interface Sci. **1997,** *70*, 171.
31. Ferraro, J.R.; Peppard, D.F.; Mason, G.W. J. Inorg. Nucl. Chem. **1965,** *27*, 2055.
32. Thomas, L.C. *Interpretation of the Infrared Spectra of Organophosphorus Compounds*; Heyden: London, 1974.
33. Moedritzer, K.; and Irani, R.R. J. Inorg. Nucl. Chem. **1961,** *22*, 297.
34. Moyer, B.A.; Baes, Jr., C.F.; Case, G.N.; Lumetta, G.J.; Wilson, N.M. Sep. Sci. Technol. **1993,** *28*, 81.
35. Neuman, R.D.; Zhou, N.F.; Wu, J.; Jones, M.A.; Gaonkar, A.G.; Park, S.J.; Agrawal, M.L. Sep. Sci. Technol. **1990,** *25*, 1655.
36. Chiarizia, R.; Danesi, P.R.; Raieh, M.A.; Scibona, G. J. Inorg. Nucl. Chem. **1975,** *37*, 1495.
37. Magid, L.J. Structure and Dynamics by Small-Angle Neutron Scattering. In *Nonionic Surfactants, Physical Chemistry;* Schick, M.J., Ed., Surfactant Science Series. Marcel Dekker, Inc.: New York, 1987; Vol. 23.
38. Thiyagarajan, P.; Diamond, H.; Danesi, P.R.; Horwitz, E.P. Inorg. Chem. **1987,** *26*, 4209.
39. Thiyagarajan, P.; Diamond, H.; Horwitz, E.P. J. Appl. Cryst. **1988,** *21*, 848.

MARCEL DEKKER, INC.
270 Madison Avenue, New York, New York 10016

40. Diamond, H.; Thiyagarajan, P.; Horwitz, E.P. Solvent Extr. Ion Exch. **1990,** *8*, 503.
41. Steytler, D.C.; Jenta, T.R.; Robinson, B.H.; Eastoe, J.; Heenan, R.K. Langmuir **1996,** *12*, 1483.
42. Nash, K.L.; Rogers, R.D.; Ferraro, J.R.; Zhang, J. Inorg. Chim. Acta **1998,** *269*, 211.

MARCEL DEKKER, INC.
270 Madison Avenue, New York, New York 10016

Request Permission or Order Reprints Instantly!